CDF note 9454

Mass Measurement of the $X(3872)$ State

The CDF Collaboration

URL http://www-cdf.fnal.gov

(Dated: July 31, 2008)

We present an analysis of the $X(3872)$ mass in its decay to $J/\psi\pi^+\pi^-$. The possibility of the existence of two nearby states is probed by comparing the expected width of one/two state hypotheses to the measured width in data. No indication for two states is found. An upper limit is set on the mass difference between two possible states, $\Delta m \leq 3.2\,(3.6)\,\mathrm{MeV}/c^2$ at 90% (95%).

The $X(3872)$ mass is precisely measured to be $m_{X(3872)} = 3871.61 \pm 0.16\,(\mathrm{stat}) \pm 0.19\,(\mathrm{syst})\,\mathrm{MeV}/c^2$. This measurement is the most precise measurement of the $X(3872)$ mass to date. The measured value is smaller than the sum of the D^0 and D^{0*} meson masses, still allowing the hypothesis for the $X(3872)$ to be a bound state of $D^0 D^{0*}$ mesons.

Preliminary Results for Summer 2008 Conferences

I. INTRODUCTION

The $X(3872)$ remains an unsolved puzzle till the present day. It was discovered by Belle in 2003 [1]. The only quark-model explanation, a charmonium state with quark content $c\bar{c}$, does not easily explain the measured properties of the $X(3872)$ [2].

Attempts have thus shifted to explain the $X(3872)$ as an exotic state. One very intriguing possibility is the explanation of the $X(3872)$ as a molecular state, composed by D^0 and D^{0*} mesons. This possibility is mostly motivated by the uncanny identity of the $X(3872)$ mass and the sum of the D^0 and D^{0*} masses. Further attempts to explain the $X(3872)$ are multiquark compositions, quark-gluon hybrids or pure glueballs. While all these possibilities are exotic, none of them is explicitly forbidden within QCD. To date, the status of the $X(3872)$ is completely undetermined. While experimental evidence is mounting, most hypotheses are still possible — this is explainable to some degree, since phenomenological models are uncertain with predictions and the status of lattice QCD calculations is developing but far from predictive as well.

Growing experimental interest in charm spectroscopy caused the discovery of further new resonances, the XYZ states. While for each single state one or another interpretation may be preferred, the big picture to accommodate all states is completely unclear [3]. The most interesting state at the moment is the $Z(4430)$ state, since it is a charged state. If confirmed, this state would unambiguously point to an exotic state, since all quark-model charmonium states are neutral. It is evident that spectroscopy may be on the verge of establishing structures beyond the common meson and baryon structures.

The $X(3872)$ in its decay mode to $J/\psi\pi^+\pi^-$ is the only XYZ state observed at CDF. A dedicated trigger to select J/ψ events, combined with a good momentum resolution allows to obtain a clear signal structure. This was already exploited by previous CDF analyses. So far the $X(3872)$ was confirmed [4] with a first measurement of its mass, the dipion mass distribution was measured [5] and the angular distribution was analyzed to determine the $X(3872)$ quantum numbers J^{PC} [6].

A very important property of the $X(3872)$ is its mass. On the one hand the value is interesting on its own because it does not agree very well with predicted charmonium masses. On the other hand and more importantly, the mass difference to the sum of the D^0 and D^{0*} masses is of interest. The picture of a bound 'molecular' state of these two mesons is very popular because of the near identity in mass between the $X(3872)$ mass and the summed D^0 and D^{0*} masses. Whether or not such a state is bound crucially depends on the question, whether the $X(3872)$ is heavier or lighter than the sum of the 'constituent' masses. In order to answer this question a precise mass determination of the $X(3872)$ is required.

Some exotic hypotheses to explain the $X(3872)$ predict a whole spectrum of exotic states out of which the $X(3872)$ is only one. The multiquark model of Maiani *et al.* [7] accommodates the $X(3872)$ as a mixture of two neutral flavor states and predicts the existence of a partner state of similar mass. This hypothesis can be tested by investigating whether the observed $X(3872)$ mass structure is compatible with two separate peaks or not.

In this document we first describe the CDF detector and the trigger system in section II. The dataset used and the candidate selection is described in section III. In section IV we describe the width study of the mass shape of the observed signal in order to determine its compatibility with being due to a single peak. The precise measurement of the $X(3872)$ mass is presented in section IV. We conclude by a short discussion of the obtained results in section VI.

II. CDF DETECTOR AND TRIGGER

The components and capabilities of the CDF II detector [8] most relevant for this analysis are the tracking system and the muon detectors. The tracking system lies within a uniform axial magnetic field of strength 1.4 T. The inner tracking volume up to a radius of 28 cm is filled with $6-7$ layers of double-sided silicon microstrip detectors [9]. An additional layer of single-sided silicon is mounted directly to the beam-pipe at a radius of 1.5 cm, providing an excellent resolution of the impact parameter d_0, defined as the distance of closest approach of the track to the interaction point in the transverse plane. The remainder of the tracking volume up to the radius of 137 cm is occupied with an open-cell drift chamber (COT)[10]. Muons are detected in planes of multi-wire drift chambers and scintillators [11] . The muon chambers are located outside the hadronic and electromagnetic calorimeters, which act as absorber material. The muon detectors used in this study cover the pseudorapidity range $|\eta| \leq 1.0$, where $\eta = -\ln\tan(\theta/2)$ and θ is the polar angle measured from the proton direction.

A three-level trigger system is used for the online event selection. The trigger components important for this analysis are the extremely fast tracker (XFT) [12], which, at level 1 of the trigger system, groups COT hits into tracks in the transverse plane. The events are selected by a dimuon trigger [8] which requires two tracks of opposite charge found by the XFT which match to a track segments in the muon chambers and have a dimuon mass consistent with the J/ψ mass.

particle candidate	requirements
pion candidate	$p_T > 0.4$ GeV$/c$ $\lvert\eta\rvert < 1$ ≥ 10 COT hits, ≥ 2 SVX hits
muon candidate	$p_T > 1.5$ GeV$/c$ $\lvert\eta\rvert < 1$ ≥ 10 COT hits, ≥ 2 SVX hits
J/ψ candidate	$2.95\,\mathrm{GeV}/c^2 < m(\mu\mu) < 3.25\,\mathrm{GeV}/c^2$ $\chi^2(\mu^+\mu^-) < 30$
$X(3872)$ candidate	$m(J/\psi\pi\pi) < 4.0\,\mathrm{GeV}/c^2$ $p_T > 3.5$ GeV$/c$ $\chi^2(J/\psi\pi\pi) < 40$

TABLE I: $X(3872)$ preselection cuts.

III. DATA SAMPLE AND SELECTION

We use data collected by the CDF II detector from February 2002 until August 2007 using the dimuon trigger. The data corresponds to an integrated luminosity of $\mathcal{L} \approx 2.4\,\mathrm{fb}^{-1}$.

In the offline reconstruction we first combine two muon candidates to a J/ψ candidate. As muon candidates we use all tracks which can be matched to a track segment in the muon detectors. The J/ψ candidate is subject to a kinematical fit with vertex constrain. Afterwards we combine the J/ψ candidate with two other tracks which are assumed to be pions to form an $X(3872)$ candidate. In the final step a kinematic fit of the $X(3872)$ candidate is performed. In this fit we constrain all four tracks to originate from a common point and the two muons forming the J/ψ are constrained to have an invariant mass equal to the world average J/ψ mass. In the reconstruction and selection process we keep a wider invariant mass region from threshold to $4.0\,\mathrm{GeV}/c^2$ to also include the $\psi(2S)$ state which we use as control sample.

The selection procedure starts with a preselection of candidates, with the main task of reducing obvious background while maintaining high signal efficiency. The requirements used in this step are listed in table I.

The next step in the selection process is performed by using a neural network. The employed neural network is the NeuroBayes package [13, 14]. The neural network combines several input quantities to form a single output quantity on which the selection is performed. The output of the neural network corresponds to a transformation from a multidimensional space of input quantities to a one-dimensional output quantity. The input quantities to the neural network are listed in table II. The transformation is chosen during a training phase in a way that it maximizes the separation between signal and background. For the training of the neural network we need two sets of events with a known classification of signal or background. The background sample is taken from data using $X(3872)$ mass sidebands defined by $[3816.7 - 3841.7;\ 3901.7 - 3926.7]\,\mathrm{MeV}/c^2$. As a signal sample we use simulated signal-only events. We generate the kinematic $X(3872)$ distributions according to measured $\psi(2S)$ distributions. The generated $X(3872)$ particles are decayed using EvtGen [15] into the $J/\psi\pi\pi$ final state assuming a ρ nature of the dipion system. After the decay each event is passed through the standard CDF detector simulation, based on the GEANT3 package. The resulting events are reconstructed with the same reconstruction software as real measured data events. In table III we give a ranking of the input quantities to the neural network. The quantities denoted as correlation significance and significance loss are calculated based on the correlation of the variables to the classification truth. To calculate the correlation significance, one calculates for each variable the correlation to the truth defined as

$$\rho^{ti} = \frac{\frac{1}{n}\sum_{j=1}^{n}\left(x_j^t - < x^t >\right)\cdot\left(x_j^i - < x^i >\right)}{\sqrt{V[x^t]V[x^i]}},$$

where t denotes the truth, i the correlated variable, $< x^i >$ the expectation value for the given variable, $V[x^i]$ its variance and n the number of events in the training sample. Then the correlation significance for a given variable is $\rho^{ti}\cdot\sqrt{n}$. For the significance loss, we first decorrelate all input quantities and than calculate the correlation between the truth and each decorrelated variable $\tilde{\rho}^{ti}$. The total correlation is then defined by

$$\rho_{TN}^2 = \sum_{i=1}^{N}\tilde{\rho}^{ti2},$$

where N is the number of variables. An analogous procedure is repeated without the considered variable to calculate

#	variable	description
1	$\chi^2(J/\psi\pi\pi)$	$J/\psi\pi\pi$ vertex fit quality
2	$p_{T,X(3872)}$	transverse momentum of the $X(3872)$ candidate
3	$\chi^2(\mu\mu)$	$\mu\mu$ vertex fit quality
4	$p_{T,J/\psi}$	transverse momentum of the J/ψ candidate
5	$m_{J/\psi}$	fitted mass of the J/ψ candidate
6	$\max(\mathrm{NN}_{\mu^+},\, \mathrm{NN}_{\mu^-})$	larger muon network probability
7	$\min(\mathrm{NN}_{\mu^+},\, \mathrm{NN}_{\mu^-})$	smaller muon network probability
8	$\max(p_{T,\mu^+},\, p_{T,\mu^-})$	larger transverse muon momentum
9	$\max(\Delta R_{\pi^+},\, \Delta R_{\pi^-})$	larger pion cone radius relative to $X(3872)$
10	$\max(m_{J/\psi\pi^+},\, m_{J/\psi\pi^-})$	larger mass of $J/\psi\pi^+$ and $J/\psi\pi^-$ systems
11	Q	Q value of the decay, $Q = m_{J/\psi\pi\pi} - m_{\pi\pi} - m_{J/\psi}$
12	$\max(p_{T,\pi^+},\, p_{T,\pi^-})$	larger transverse momentum of pion
13	$\min(p_{T,\pi^+},\, p_{T,\pi^-})$	smaller transverse momentum of pion
14	$\lvert\eta_\pi,\mathrm{mean}\rvert$	absolute average pion pseudorapidity

TABLE II: Input quantities for the $X(3872)$ selection network. The muon network probability is the output of a dedicated neural network and gives an estimate whether a particle is a muon or not.

rank	variable	correlation significance	significance loss
1	Q	465.65	336.19
2	$\max(p_{T,\pi^+},\, p_{T,\pi^-})$	268.04	80.84
3	$\chi^2(J/\psi\pi\pi)$	210.42	125.64
4	$\min(\mathrm{NN}_{\mu^+},\, \mathrm{NN}_{\mu^-})$	111.59	69.66
5	$\min(p_{T,\pi^+},\, p_{T,\pi^-})$	77.42	52.70
6	$p_{T,J/\psi}$	46.84	8.66
7	$m_{J/\psi}$	39.55	37.13
8	$\max(\mathrm{NN}_{\mu^+},\, \mathrm{NN}_{\mu^-})$	28.82	28.40
9	$\max(\Delta R_{\pi^+},\, \Delta R_{\pi^-})$	19.57	19.33
10	$\chi^2(\mu\mu)$	14.86	14.85
11	$\lvert\eta_\pi,\mathrm{mean}\rvert$	10.89	10.97
12	$\max(p_{T,\mu^+},\, p_{T,\mu^-})$	6.69	7.19
13	$\max(m_{J/\psi\pi^+},\, m_{J/\psi\pi^-})$	6.51	6.54
14	$p_{T,X(3872)}$	4.11	4.11

TABLE III: Ranking of the input quantities for the $X(3872)$ selection network.

ρ^2_{TN-1}. The significance loss is then given by

$$\sqrt{\rho^2_{TN} - \rho^2_{TN-1}} \cdot \sqrt{n}.$$

Intuitively, the correlation significance is proportional to the amount of information which is provided by a given quantity without all others while the significance loss corresponds to the amount of information lost for the neural network if we remove the given quantity while we keep all others. The two quantities adding most of the information to the separation power are the Q value and $\chi^2(J/\psi\pi\pi)$. In Fig. 1 we show the distribution of the neural network output separately for the signal and the background distribution from the training sample.

In the last selection step requirements are placed on the neural network output (NN) and the number of candidates per detector event (N_{cand}). For the number of candidates we count all right-sign candidates which pass the preselection requirements listed in table I. The requirement on the neural network output is chosen by maximizing the quantity $S_1 = N_{MC}/\sqrt{N_{data}}$, where N_{MC} is the number of events selected in the simulated sample and N_{data} is the number of events selected in a ± 10 MeV/c^2 window around a mass of 3871.7 MeV/c^2. The dependence of S_1 from the requirement on the neural network output is shown in Fig. 2. Based on Fig. 2 we choose to select events which have a neural network output greater than 0.25. In Fig. 3 we show the invariant mass distribution of selected and removed candidates. After we choose the requirement on the neural network output we choose the requirement on the number of candidates, using the sample selected by the requirement on the neural network. For this selection we rely solely on data, as we do not simulate the underlying event in our simulation sample. We again maximize the significance, this time defined as $S_2 = N_S/\sqrt{N_S + N_B}$ where N_S and N_B are the number of signal and background events in data in a ± 10 MeV/c^2 window around the nominal $X(3872)$ mass for a given requirement. To estimate N_S and N_B we fit the invariant mass distribution with a second order polynomial to describe the combinatorial background and a Gaussian

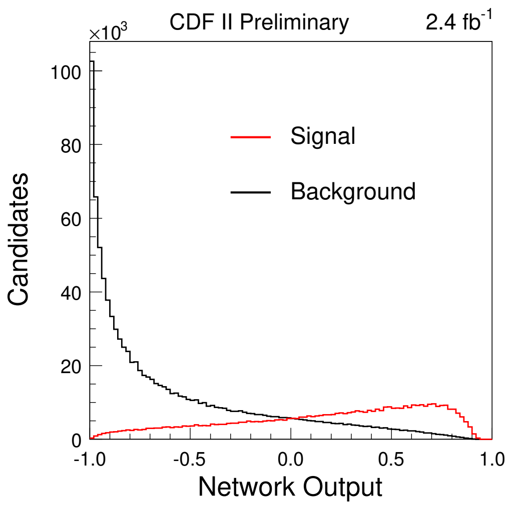

FIG. 1: Distribution of the neural network output for signal and background from the training sample.

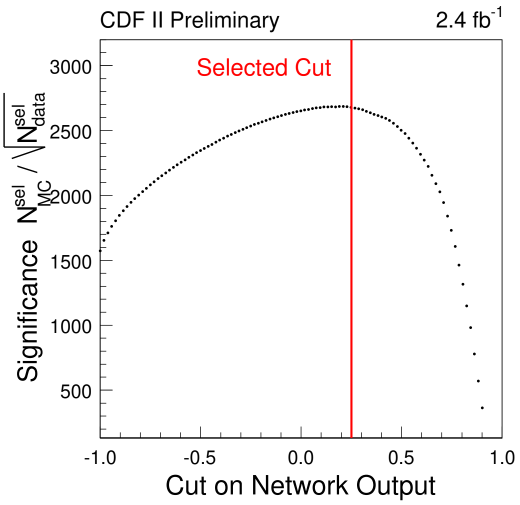

FIG. 2: Dependence of $S_1 = N_{MC}/\sqrt{N_{data}}$ on the requirement on the neural network output.

function to describe the signal. The dependence of S_2 on the requirement that the number of candidates is smaller than given value is shown in Fig. 4. For our final selection we retain events which have a number of candidates less or equal to three. In Fig. 5 we show the invariant mass after the neural network selection, both for the candidates selected by the requirement on the number of candidates and those which are removed. In the final sample we select around 34500 $\psi(2S)$ and 6000 $X(3872)$ signal events.

IV. $X(3872)$ MASS SHAPE STUDY

Multiquark hypotheses are among the most prominent models to explain the $X(3872)$. In most cases they do not only accommodate the $X(3872)$, but also predict a spectrum of different states. In many models the $X(3872)$ is described by a combination of two charm quarks with two light quarks. Because multiple combinations of light quarks are possible, also multiple $X(3872)$-like states with similar mass are possible.

If the multiquark hypothesis holds for the $X(3872)$, it is thus possible that the observed $X(3872)$ enhancement in the $J/\psi\pi^+\pi^-$ mass spectrum is in reality not only one peak, but rather an unresolved structure of two peaks. This hypothesis can to some extent be valid for the earlier confirmations of the $X(3872)$ at CDF, since the mass resolution of the measurement is of the order of $5\,\mathrm{MeV}/c^2$. However, also the B-factories with better resolution only observe one peak. Maiani *et al.* explain this behavior in their multiquark model [7, 16]. It is suggested that only one of the

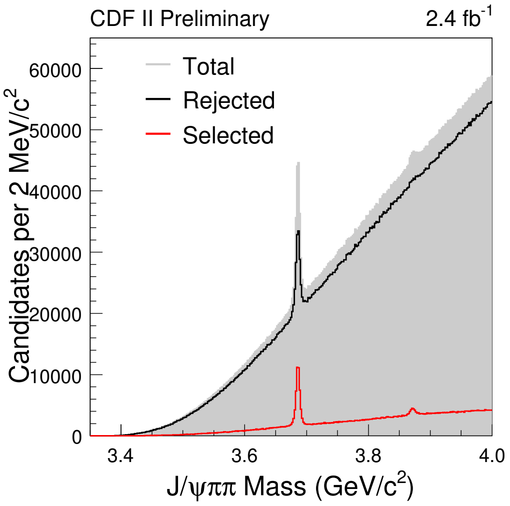

FIG. 3: Invariant mass distribution for events selected by the requirement that the neural network output is greater than 0.25 (red), and of events removed by this requirement (black).

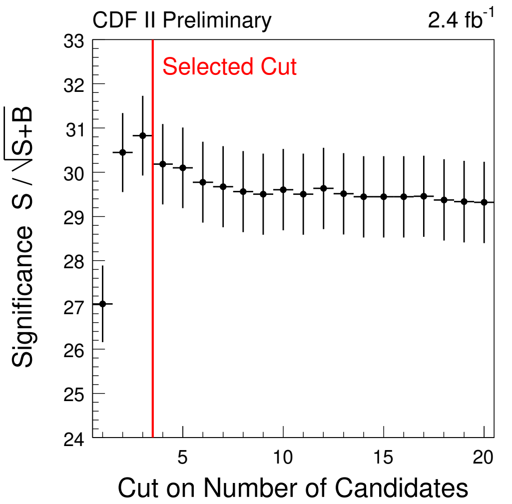

FIG. 4: Dependence of $S_2 = N_S/\sqrt{N_S + N_B}$ on the requirement that the number of candidates is smaller than a given value.

neutral multiquark states is predominantly produced in the observed decay of a charged b-meson, i.e. in the decay $B^+ \to X(3872)K^+$. The other neutral state is produced in the decay of a neutral b-meson $B^0 \to X(3872)K^0_S$.

At the Tevatron, the $X(3872)$ production via the decay of b-mesons is small compared to the one from direct fragmentation. As a consequence, both neutral states should be observable at the same time in the decay to $J/\psi\pi^+\pi^-$. If the mass difference of two states is smaller or of the order of the detector mass resolution, they cannot be clearly separated. However, it is still possible to draw conclusions which allow to answer the question whether the description of the measured signal requires two separate states or if one state suffices.

It will be tested whether the observed peak at the $X(3872)$ mass is due to a single state or two states with a small mass difference. The basic idea behind this test is that a peak due to two states will appear wider than due to only one state. Thus when we fit a mass distribution with a function which uses a certain dispersion parameter, for two states the dispersion parameter will get on average larger than for a single state. The dispersion parameter then can be used as a test statistics. The test is performed by measuring the dispersion parameter in data and compare it to the expectations for various hypotheses.

In case the peak is due to a single state we would describe it by a Breit-Wigner function convoluted with a resolution function. Such a model is a good starting point to construct our test statistics as it has a dispersion parameter. In the actual procedure we fix the width of the Breit-Wigner function as well as the resolution to our expectations and introduce a single scaling parameter, which scales both the natural width and the resolution. This scaling parameter

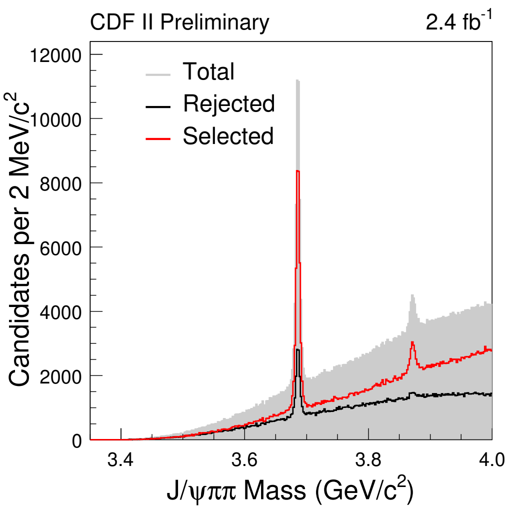

FIG. 5: The invariant mass distribution for events selected by the requirement on the number of candidates (red) and of events removed by the requirement (black).

is left floating in the fit to data and is then used as test statistics.

The fit model we use to describe the data is composed of a second order polynomial to describe the combinatorial background and a non-relativistic Breit-Wigner function convolved with a resolution function to describe the signal. The resolution function is phenomenologically parameterized by two Gaussian functions with common mean yielding a signal function of

$$y_S(m; m_0, f_n, t, \sigma_n, k, \Gamma) = f_n \,\mathrm{Voigt}(m; m_0, t\cdot\sigma_n, t\cdot\Gamma) \;+\; (1-f_n)\,\mathrm{Voigt}(m; m_0, t\cdot k\sigma_n, t\cdot\Gamma).$$

Here f_n is the fraction of events in the core (narrower Gaussian) of the resolution distribution, σ_n is the width of this core, k is a multiplicative factor which parameterizes how much wider the tail of resolution function is compared to the core, Γ is the natural width of the state and t is the scaling parameter used as test statistics. In a binned maximum likelihood fit Γ, k, f_n and σ_n are fixed to the expectation. For the natural width Γ we use the average of measurements available from the B-factories, $\Gamma = 1.34$ MeV [1, 17]. The resolution parameters are obtained from simulation and corrected for the difference between simulation and data observed in the decay $\psi(2S) \to J/\psi\pi\pi$.

To obtain the expectation for the test statistics t for different hypotheses, we create ensembles of generated experiments, which we fit in the same manner as data. Each hypothesis is given by two parameters. Those are the mass difference Δm of the two states and the fraction of the lower mass state f_1 to the overall contribution of the observed signal. The null hypothesis with a single state contributing to the observed signal is a special case with $\Delta m = 0$, for which f_1 is completely arbitrary. Samples are generated using the polynomial background and two sets of functions y_S with mean masses chosen in a way that their mean is equal to the $X(3872)$ mass. Some of the parameters are not known with absolute precision. Those are varied in the process of the sample generation to account for uncertainties. Varied parameters are the shape of the background, the number of signal and background events, the resolution σ_n and the natural width Γ. The background shape parameters and the number of signal and background events are varied according to their statistical uncertainties from the fit to data. The core resolution σ_n is varied according to the resolution uncertainties, based on the comparison of $\psi(2S)$ data measurements to a simulated sample using the full CDF detector simulation. The natural width can be obtained from the measured values from the B-Factories with a precision of 0.64 MeV. Therefore we vary Γ according to a Gaussian distribution with width equal to 0.64 MeV while constraining Γ to be positive. In addition we assume that both contributing states have the same natural width.

In Fig. 6 we show the distribution of the scale t for the hypothesis that the signal in data is entirely due to a single state (or two states with same masses). Comparing this distribution to the value measured in data, $t = 1.052$, we conclude that our data is very well compatible with a single state and that we have no evidence for two states. Therefore we set a limit on a maximum mass difference between two states, using the assumptions from the ensemble generation (two non-interfering states with same natural width). To obtain the upper limit on the mass difference we calculate p-values defined as the fraction of experiments having a scale t equal or smaller than seen in data for different Δm hypothesis. The 90% (95%) confidence level limit then corresponds to a p-value of 10% (5%). In Fig. 7 we show the expected distributions for $f_1 = 0.5$ hypotheses of the scale t for $\Delta m = 3.2$ MeV/c^2 and $\Delta m = 3.6$

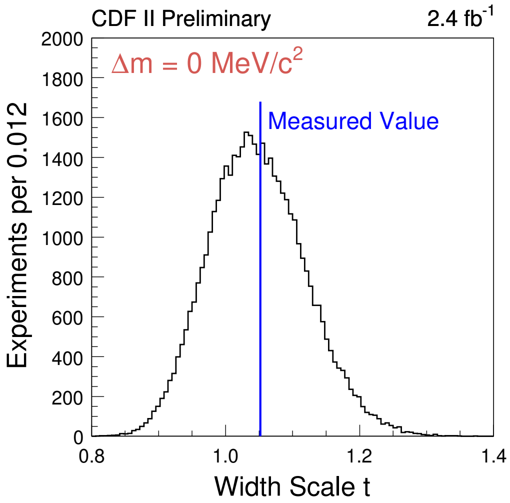

FIG. 6: Distribution of the scale t for generated experiments using the single state hypothesis (histogram). Also shown is the measured value from data (blue line).

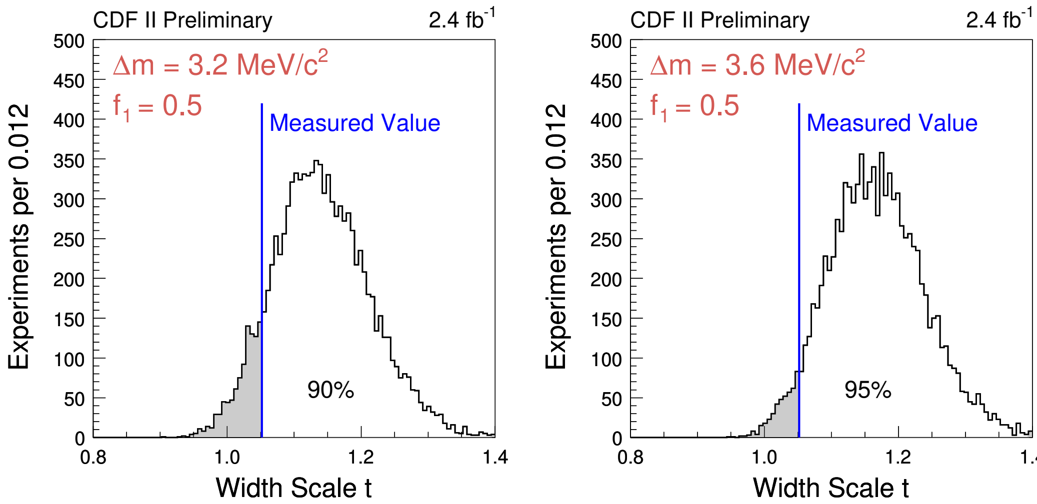

FIG. 7: Distributions of the scale t for generated experiments using $\Delta m = 3.2$ MeV/c^2 (left) and $\Delta m = 3.6$ MeV/c^2 (right) and $f_1 = 0.5$. The blue line shows the value measured in data. The shaded region corresponds to a fraction of 10% (left) and 5% (right). The two cases correspond to the 90% and 95% confidence level upper limits.

MeV/c^2, corresponding to 90% and 95% confidence level limits. In Fig. 8 we show the scale t, below which 10% (5%) of generated experiments for different Δm hypotheses are. From the scale $t = 1.052$ measured in data we set limits of $\Delta m = 3.2$ MeV/c^2 and $\Delta m = 3.6$ MeV/c^2 at 90% and 95% confidence level limits, assuming $f_1 = 0.5$. In Fig.9 we show the dependence of the upper limits on the fraction f_1 of the lower mass state.

V. $X(3872)$ MASS MEASUREMENT

Since we determined that the observed signal is compatible with the hypothesis of stemming from a single state, we can proceed to the mass measurement of this state. The mass is extracted from an unbinned maximum likelihood fit using the same fit model as used in the shape study. In this fit we fix $\Gamma = 1.34$ MeV and the expected resolution parameters. Free parameters in the fit are two parameters determining the background shape, the fraction of signal events in the sample, the width scale t, and of course the mass of the state. The fit yields

$$m(X(3872)) = 3871.61 \pm 0.16\,\mathrm{MeV}/c^2.$$

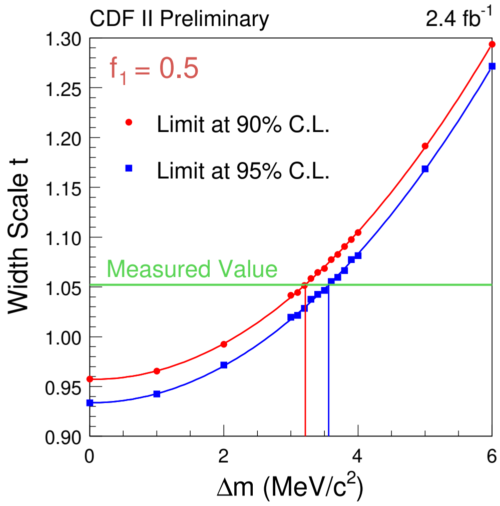

FIG. 8: Dependence of the scale t, below which 10% and 5% of generated experiments is found, on the Δm hypothesis assuming an equal mixture of two states. The horizontal line corresponds to the value measured in data and the two vertical lines indicate the 90% and 95% upper limits we set.

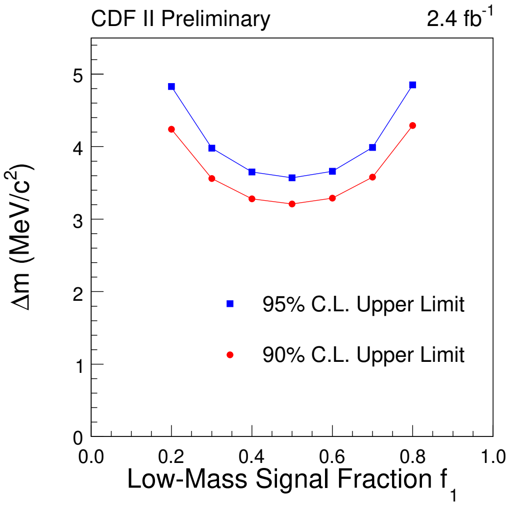

FIG. 9: Dependence of the upper limit on the mass difference Δm between two states on the fraction f_1.

In Fig. 10 we show a projection of the fit.

As main sources of systematic uncertainties we investigate uncertainties in the fit model and the momentum scale. To estimate the effect due to the uncertainties in the fit model we refit the data using alternative models. Those include the use of a linear function instead of a second order polynomial for the background description, a single Gaussian function instead of a non-relativistic Breit-Wigner function convoluted with double Gaussian resolution function for the signal description, and fixing the natural width Γ to zero or twice the default value. We also performed a fit in mass windows reduced by 40%. All of these modifications have negligible effect on the fitted mass, and therefore we don't assign any systematic uncertainty to the fit model.

To estimate the uncertainty due to the calibration of the momentum scale we use the decay $\psi(2S) \to J/\psi\pi\pi$ which is close to the $X(3872)$ state. We use the same fit model as for the $X(3872)$, with the exception that the signal shape parameters are adjusted to the world average value of $\Gamma = 0.337$ MeV$/c^2$ [18] for the intrinsic width and that resolution parameters are adjusted to values at the $\psi(2S)$ mass. The fit projection is shown in Fig. 11. This fit yields

$$m(\psi(2S)) = 3686.03 \pm 0.02\,\mathrm{MeV}/c^2,$$

which is in excellent agreement with the world average value of

$$m^{WA}(\psi(2S)) = 3686.09 \pm 0.03\,\mathrm{MeV}/c^2.$$

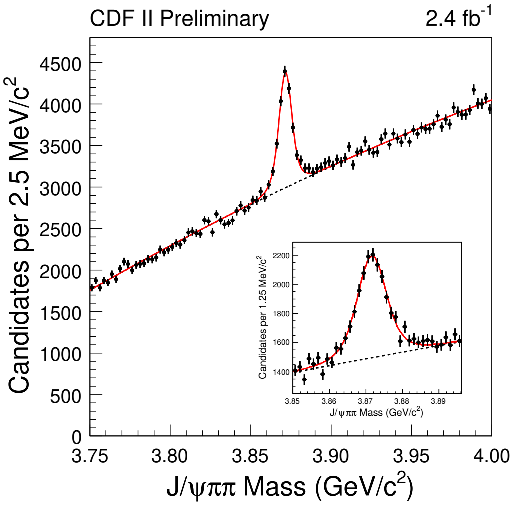

FIG. 10: Projection of the unbinned maximum likelihood fit for the mass measurement of the $X(3872)$. The points represent data, the full line the total fit and the dashed line the combinatorial background. An inset shows a zoom to the region of the $X(3872)$.

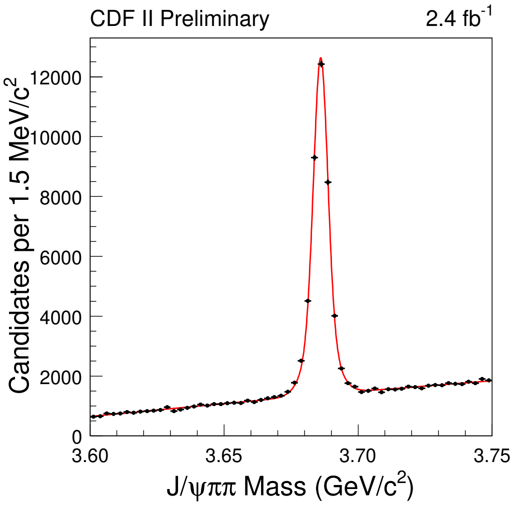

FIG. 11: Projection of the unbinned maximum likelihood fit for the mass measurement of $\psi(2S)$. The points represent data and the full line the total fit.

While there is no evidence that the $\psi(2S)$ mass would differ from the world average value we use the difference between our measurement and world average value of 60 keV as an estimate of a possible uncertainty due to both uncertainties in our measurement and the world average value.

As a possible miscalibration of the momentum scale would show up as a dependence of the measured mass on momentum, we measure the $\psi(2S)$ mass as a function of several kinematical variables. In Figs. 12 to 15 we show the deviation of the $\psi(2S)$ mass in bins of transverse momentum of all particles involved in the decay to the value from the integrated sample. We conclude that any possible effect is below 0.1 MeV/c^2 which we take as a measure of the systematic uncertainty.

To translate the estimate on the momentum scale from the $\psi(2S)$ to the $X(3872)$ we first add the two contributions in quadrature and then scale it up by the ratio of Q values of the $\psi(2S)$ and the $X(3872)$. This yields a total systematic uncertainty of 0.19 MeV/c^2. The final mass measurement for the $X(3872)$ thus is

$$m(X(3872)) = 3871.16 \pm 0.16(\text{stat}) \pm 0.19(\text{sys})\ \text{MeV}/c^2.$$

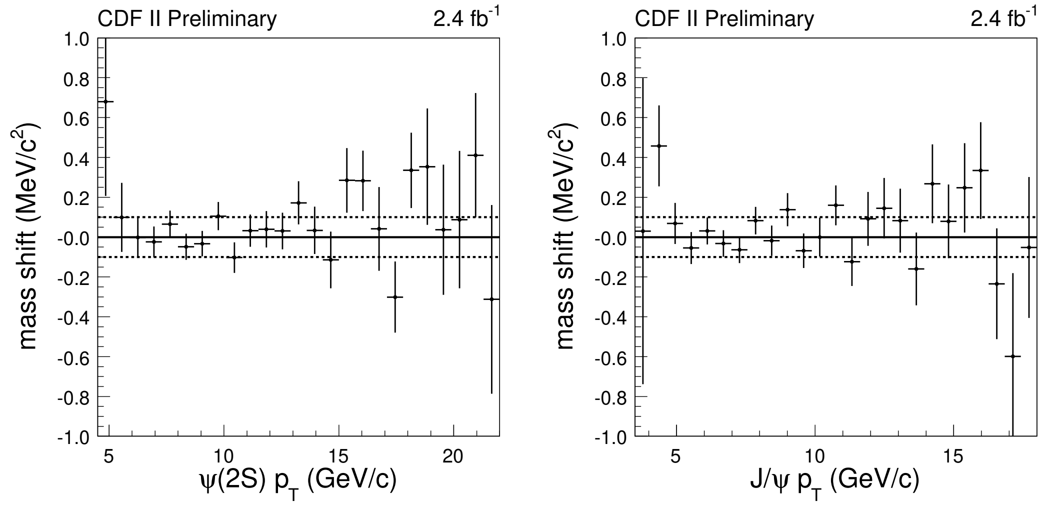

FIG. 12: Dependence of the $\psi(2S)$ mass on transverse momenta of $\psi(2S)$ (left) and transverse momenta of J/ψ (right). Shown on the y-axis is the difference to the result for the integrated sample.

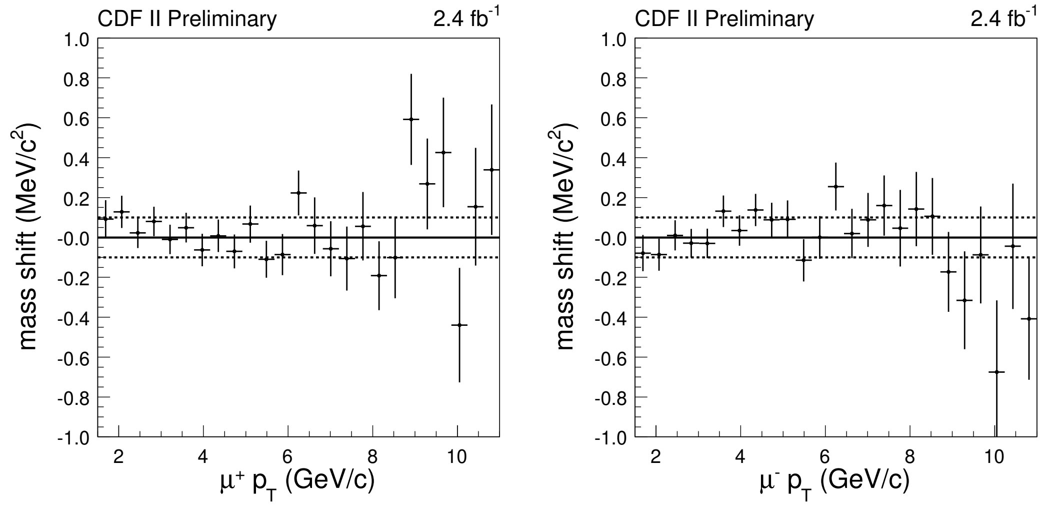

FIG. 13: Dependence of the $\psi(2S)$ mass on transverse momenta of μ^+ (left) and transverse momenta of μ^- (right). Shown on the y-axis is the difference to the result for the integrated sample.

VI. DISCUSSION

The observed peak structure agrees well with the expectations for only one state. This confirms the results from Belle and *BABAR* [17, 19] with high statistical power. They measure the $X(3872)$ mass both in B^+ and B^0 decays. While the statistically very weak result from *BABAR* indicates a 2σ mass deviation in the B^0 decay (also see figure 16), the Belle result shows essentially no deviation, but also with low statistical power.

The measured mass of $m_{X(3872)} = 3871.61 \pm 0.16\ (\mathrm{stat}) \pm 0.19\ (\mathrm{syst})\ \mathrm{MeV}/c^2$ is well consistent with the current world average value $m_{PDG} = 3871.4 \pm 0.6\,\mathrm{MeV}/c^2$ [20]. This new measurement has by far the lowest measurement uncertainty of all single $X(3872)$ mass measurements and will dominate the world average $X(3872)$ mass. Figure 16 shows the impact of the measured $X(3872)$ mass. Shown are the most recent mass measurements from the single experiments, combined to a world average. Compared to the world average from the Particle Data Group the mass measurement of the $X(3875)$ is omitted, since it is not clear whether this state is connected to the $X(3872)$ or not. This results in a world average mass of $3871.20 \pm 0.39\mathrm{MeV}/c^2$ without the new measurement of this analysis. Replacing the old CDF measurement with the new one results in an average of $m = 3871.51 \pm 0.22\,\mathrm{MeV}/c^2$, shifting the value by $0.3\,\mathrm{MeV}/c^2$ to higher masses and reducing the uncertainty of the world average mass by almost a factor of 2.

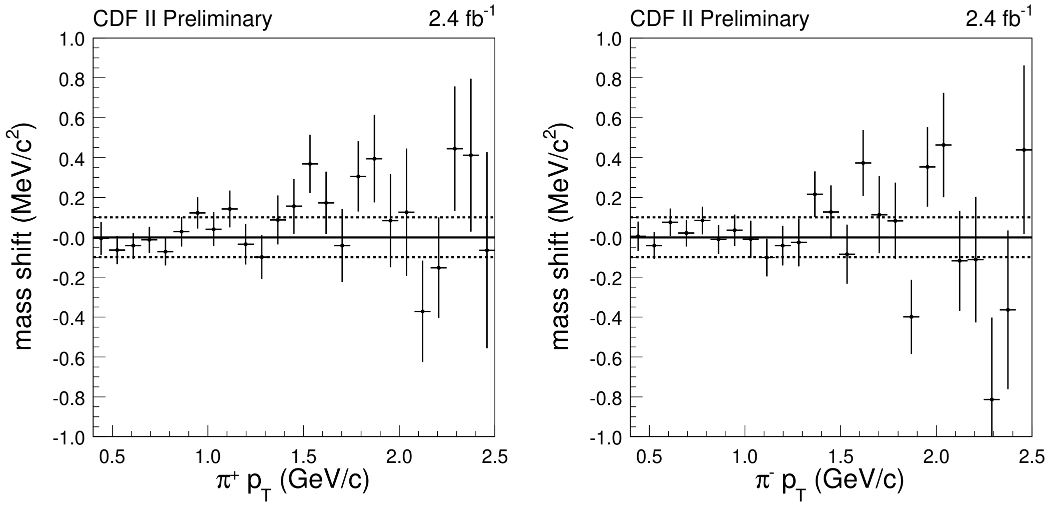

FIG. 14: Dependence of the $\psi(2S)$ mass on transverse momenta of π^+ (left) and transverse momenta of π^- (right). Shown on the y-axis is the difference to the result for the integrated sample..

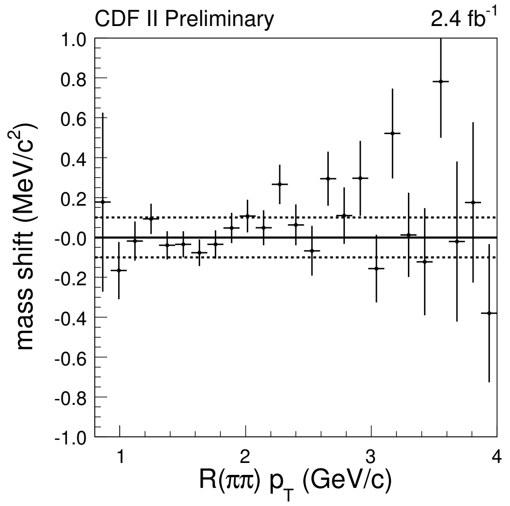

FIG. 15: Dependence of the $\psi(2S)$ mass on the transverse momentum of the dipion system.

It is further possible to use this new measurement to derive a limit on the mass difference between two possible states. It is assumed that the B-factories only produce one of the states with mass $m_+ = 3871.55 \pm 0.50$ MeV/c^2 in the B^+ decay channel, while CDF observes a mixture of these states with combined mass $m_{CDF} = 3871.61 \pm 0.25$ MeV/c^2 where the state seen by the B-factories contributes the fraction f_+ to the signal seen by CDF. Then it can be shown, that the mass difference between the states is given by the relation $\Delta m = (m_+ - m_{CDF})/(1 - f_+)$. Using both mass measurements this can be translated into a limit, depending on the ratio of states seen at CDF. If at CDF the same state as observed at the B-factories is dominantly produced (f_+ close to 1), then the limit is very weak. If CDF however produces the other state more dominantly, then the limit becomes very good. This behavior is illustrated in figure 17.

The mass measurement and the limit on a possible mass splitting together with the measurement of the quantum numbers are important contributions to understand the nature of the $X(3872)$. The hypothesis $J^{PC} = 1^{++}$ agrees with the ground state prediction of 'molecular' $D^0\bar{D}^{0*}$ bound state models. The performed precise mass measurement of the $X(3872)$ adds crucial information to this hypothesis. By comparing the central value of the average to the world average value of the sum of the 'molecular constituents', $m_{D^0D^{0*}} = 3871.81\,\mathrm{MeV}/c^2$, it can be seen that the $X(3872)$ is lighter by $0.3 \pm 0.4\,\mathrm{MeV}/c^2$. This still allows for a simple bound state. Unfortunately, the involved uncertainty does not allow to firmly determine the heavier system. With the new $X(3872)$ mass measurement, this uncertainty is now dominated by the uncertainties on the D masses.

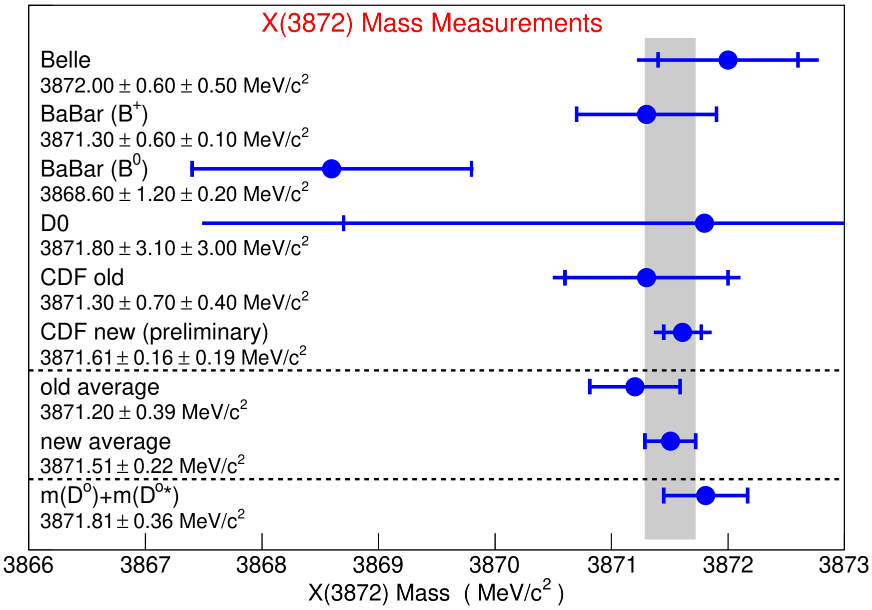

FIG. 16: An overview of the measured $X(3872)$ masses from the experiments observing the $X(3872)$. Shown are the measurement from Belle [1], *BABAR* (from both B^+ and B^0 decays) [17], DØ [21], and the first CDF measurement [4]. The result from this analysis is shown as the last single measurement entry. Additionally shown is the change in the world average mass due to the new measurement. The current value for the D^0D^{0*} threshold is shown as the last entry. Shown are the statistical and combined errors on each measurement.

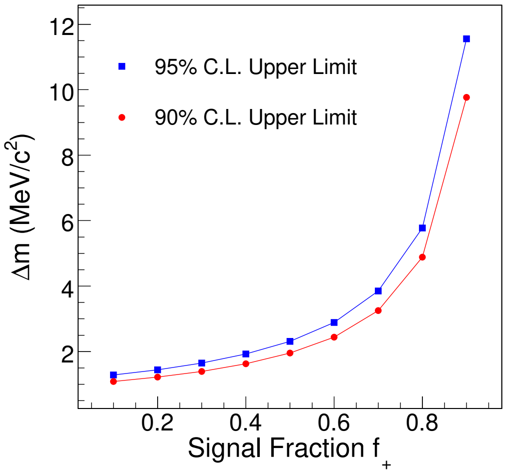

FIG. 17: The limit on the mass difference between two possible X-states, combining the masses from the B-factories in the B^+ decay channel and the new CDF measurement.

The quantum numbers $J^{PC} = 1^{++}$ agree with the prediction of various multiquark models. The model of Maiani *et al.* is however disfavored, since there is no evidence for two separate states. The proposed mass difference of $(8 \pm 3)\,\mathrm{MeV}/c^2$ is beyond the obtained upper limits for the mass difference. This either means that there simply is no prominent second neutral state decaying into $J/\psi\pi^+\pi^-$ or that the two possible states are so close in mass that they cannot be resolved by experiment. While multiquark hypotheses remain an interesting field, no model with verifiable predictions has so far turned out to be correct.

In summary we present a new measurement of the $X(3872)$ mass using the decay to $J/\psi\pi^+\pi^-$. The measured value $m_{X(3872)} = 3871.61 \pm 0.16\,(\mathrm{stat}) \pm 0.19\,(\mathrm{syst})\,\mathrm{MeV}/c^2$ is the most precise measurement to date and consistent with previous measurements in the same decay channel. In addition we derive an upper limit on the mass difference for the hypothesis of two X states which are predicted by some multiquark scenarios.

Acknowledgments

We thank the Fermilab staff and the technical staffs of the participating institutions for their vital contributions. This work was supported by the U.S. Department of Energy and National Science Foundation; the Italian Istituto Nazionale di Fisica Nucleare; the Ministry of Education, Culture, Sports, Science and Technology of Japan; the Natural Sciences and Engineering Research Council of Canada; the National Science Council of the Republic of China; the Swiss National Science Foundation; the A.P. Sloan Foundation; the Bundesministerium für Bildung und Forschung, Germany; the Korean Science and Engineering Foundation and the Korean Research Foundation; the Science and Technology Facilities Council and the Royal Society, UK; the Institut National de Physique Nucleaire et Physique des Particules/CNRS; the Russian Foundation for Basic Research; the Ministerio de Educación y Ciencia and Programa Consolider-Ingenio 2010, Spain; the Slovak R&D Agency; and the Academy of Finland.

---

[1] S. K. Choi et al. [Belle Collaboration]. Observation of a New Narrow Charmonium State in Exclusive $B^{\pm} \to K^{\pm}\pi^{+}\pi^{-}J/\psi$ Decays. *Phys. Rev. Lett.*, 91:262001, 2003, arXiv:hep-ex/0309032.

[2] Stephen L. Olsen [Belle Collaboration]. Search for a Charmonium Assignment for the $X(3872)$. *Int. J. Mod. Phys.*, A20:240–249, 2005, arXiv:hep-ex/0407033.

[3] Stephen Godfrey and Stephen L. Olsen. The Exotic XYZ Charmonium-like Mesons. 2008, arXiv:0801.3867 [hep-ph].

[4] Darin E. Acosta et al. [CDF II Collaboration]. Observation of the Narrow State $X(3872) \to J/\psi\pi^{+}\pi^{-}$ in $\bar{p}p$ Collisions at $\sqrt{s} = 1.96$ TeV. *Phys. Rev. Lett.*, 93:072001, 2004, arXiv:hep-ex/0312021.

[5] A. Abulencia et al. [CDF Collaboration]. Measurement of the Dipion Mass Spectrum in $X(3872) \to J/\psi\pi^{+}\pi^{-}$ Decays. *Phys. Rev. Lett.*, 96:102002, 2006, arXiv:hep-ex/0512074.

[6] A. Abulencia et al. [CDF Collaboration]. Analysis of the Quantum Numbers J^{PC} of the $X(3872)$. *Phys. Rev. Lett.*, 98:132002, 2007, arXiv:hep-ex/0612053.

[7] L. Maiani, F. Piccinini, A. D. Polosa, and V. Riquer. Diquark-antidiquarks with Hidden or Open Charm and the Nature of $X(3872)$. *Phys. Rev.*, D71:014028, 2005, arXiv:hep-ph/0412098.

[8] Darin E. Acosta et al. [CDF Collaboration]. Measurement of the J/ψ Meson and $b-$hadron Production Cross Sections in $p\bar{p}$ Collisions at $\sqrt{s} = 1960$ GeV. *Phys. Rev.*, D71:032001, 2005, arXiv:hep-ex/0412071.

[9] Christopher S. Hill [On behalf of the CDF Collaboration]. Operational Experience and Performance of the CDF II Silicon Detector. *Nucl. Instrum. Meth.*, A530:1–6, 2004.

[10] Anthony Allen Affolder et al. [CDF Collaboration]. CDF Central Outer Tracker. *Nucl. Instrum. Meth.*, A526:249–299, 2004.

[11] G. Ascoli et al. CDF Central Muon Detector. *Nucl. Instrum. Meth.*, A268:33, 1988.

[12] Evelyn J. Thomson et al. Online Track Processor for the CDF Upgrade. *IEEE Trans. Nucl. Sci.*, 49:1063–1070, 2002.

[13] M. Feindt and U. Kerzel. The NeuroBayes Neural Network Package. *Nucl. Instrum. Meth.*, A559:190–194, 2006.

[14] M. Feindt. A Neural Bayesian Estimator for Conditional Probability Densities, 2004.

[15] D. J. Lange. The EvtGen Particle Decay Simulation Package. *Nucl. Instrum. Meth.*, A462:152–155, 2001.

[16] L. Maiani, A. D. Polosa, and V. Riquer. Indications of a Four-Quark Structure for the $X(3872)$ and $X(3876)$ Particles from Recent Belle and *BABAR* Data. *Phys. Rev. Lett.*, 99:182003, 2007, arXiv:0707.3354 [hep-ph].

[17] B. Aubert et al. [BABAR Collaboration]. A study of $B \to X(3872)K$, with $X(3872)- > J/\psi\pi^{+}\pi^{-}$. 2008, arXiv:0803.2838 [hep-ex].

[18] W. M. Yao et al. [Particle Data Group Collaboration]. Review of Particle physics. *J. Phys.*, G33:1–1232, 2006.

[19] BELLE-CONF-0711, First Conference Mention of the Result is: Faccini, R., Heavy Quarkonium Spectroscopy, Lepton Photon 2007, Daegu, Korea.

[20] W. M. Yao et al. [Particle Data Group Collaboration]. Review of Particle Physics. *J. Phys.*, G33:1–1232, 2006. And 2007 Partial Update for the 2008 edition.

[21] V. M. Abazov et al. [D0 Collaboration]. Observation and Properties of the $X(3872)$ Decaying to $J/\psi\pi^{+}\pi^{-}$ in $p\bar{p}$ Collisions at $\sqrt{s} = 1.96$ TeV. *Phys. Rev. Lett.*, 93:162002, 2004, arXiv:hep-ex/0405004.